Influence of adatom migration on wrinkling morphologies of AlGaN/GaN micro-pyramids grown by selective MOVPE*

Jie Chen(陈杰)[1], Pu-Man Huang(黄溥曼)[1], Xiao-Biao Han(韩小标)[1], Zheng-Zhou Pan(潘郑州)[1], Chang-Ming Zhong(钟昌明)[1], Jie-Zhi Liang(梁捷智)[1], Zhi-Sheng Wu(吴志盛)[1,2], Yang Liu(刘扬)[1,2,3,†], and Bai-Jun Zhang(张佰君)[1,2,‡]

[1] *School of Electronics and Information Technology, Sun Yat-sen University, Guangzhou* 510275, *China*
[2] *State Key Laboratory of Optoelectronic Materials and Technologies, Sun Yat-sen University, Guangzhou* 510275, *China*
[3] *Institute of Power Electronics and Control Technology, Sun Yat-sen University, Guangzhou* 510275, *China*

(Received 29 November 2016; revised manuscript received 12 February 2017; published online 20 April 2017)

GaN micro-pyramids with AlGaN capping layer are grown by selective metal–organic–vapor phase epitaxy (MOVPE). Compared with bare GaN micro-pyramids, AlGaN/GaN micro-pyramids show wrinkling morphologies at the bottom of the structure. The formation of those special morphologies is associated with the spontaneously formed AlGaN polycrystalline particles on the dielectric mask, owing to the much higher bond energy of Al–N than that of Ga–N. When the sizes of the polycrystalline particles are larger than 50 nm, the uniform source supply behavior is disturbed, thereby leading to unsymmetrical surface morphology. Analysis reveals that the scale of surface wrinkling is related to the migration length of Ga adatoms along the AlGaN $\{1\bar{1}01\}$ facet. The migration properties of Al and Ga further affect the distribution of Al composition along the sidewalls, characterized by the μ-PL measurement.

Keywords: metal–organic–vapor phase epitaxy, selective area growth, migration length

PACS: 81.05.Ea, 81.15.Gh, 81.16.Rf, 47.57.ef **DOI:** 10.1088/1674-1056/26/6/068101

1. Introduction

AlGaN and the relevant III–N compound semiconductors are considered to be ideal materials of light-emitting diodes (LEDs), laser diodes (LDs), and photodetectors covering the ultraviolet (UV) region due to their direct energy band gaps ranging from 3.4 eV to 6.2 eV.[1–4] The wide adjustable emission range of AlGaN-based opto-electrons has a great many applications in water purification, disinfection/sterilization, medicine, and biochemistry.[5,6]

Although the AlGaN epitaxial growth has already been studied for several years, it is still a challenge to grow high-quality, thick AlGaN epilayers with low threading dislocation (TD) density.[7,8] In addition, the conventional devices on *c*-plane AlGaN are strongly affected by spontaneous and piezoelectric polarization. Therefore, the hexagonal AlGaN micro-pyramid prepared by selective area growth (SAG) technique is thought as a kind of promising building block for reducing the TD[9,10] and suppressing the undesirable polarization effect.[11,12] Although high quality GaN pyramid has been successfully realized by SAG technology in a metal–organic–vapor phase epitaxy (MOVPE) system,[13–15] the SAG of AlGaN pyramids has been a challenge so far because Al adatoms cannot diffuse along a long distance and it is easy to form the nucleation of AlGaN spontaneously on dielectric surface in the environment of nitrogen due to the high bond energy of Al–N.[16] Thus, it is difficult to realize a hexagonal AlGaN micro-pyramid at the mask openings grown by selective area MOVPE, particularly for the high Al composition. But, it may be feasible to form AlGaN/GaN hexagonal pyramidal structure when growing an AlGaN capping layer on a GaN pyramid. Several studies have already been conducted, and the AlGaN/GaN micro-pyramid structure with polycrystalline particles on the mask has been obtained.[17–19] However, due to the effects of migration length of Al and Ga adatoms, the scale of pyramid is still small and the composition of AlGaN pyramid is nonuniform. Therefore, it is meaningful to clarify the migration length of adatoms along a specific crystal facet for growing the selective AlGaN pyramid. Besides, dur-

*Project supported by the National Natural Science Foundation of China (Grant Nos. 61274039 and 61574173), the National Key Research and Development Program, China (Grant No. 2016YFB0400105), the International Science and Technology Collaboration Program of Guangdong Province, China (Grant No. 2013B051000041), the International Science and Technology Collaboration Program of Guangzhou City, China (Grant No. 2016201604030055), the National High Technology Research and Development Program of China (Grant No. 2014AA032606), Guangdong Provincial Natural Science Foundation, China (Grant No. 2015A030312011), the Science & Technology Plan of Guangdong Province, China (Grant Nos. 2015B090903062, 2015B010132007, and 2015B010129010), the Science and Technology Plan of Guangzhou, China (Grant No. 201508010048), the Science and Technology Plan of Foshan, China (Grant No. 201603130003), Guangdong–Hong Kong Joint Innovation Project of Guangdong Province, China (Grant No. 2014B050505009), and the Opened Fund of the State Key Laboratory on Integrated Optoelectronics (Grant No. IOSKL2014KF17), the Zhuhai Key Technology Laboratory of Wide Bandgap Semiconductor Power Electronics, Sun Yat-sen University (Grant No. 20167612042080001).

†Corresponding author. E-mail: liuy69@mail.sysu.edu.cn
‡Corresponding author. E-mail: zhbaij@mail.sysu.edu.cn

© 2017 Chinese Physical Society and IOP Publishing Ltd

ing AlGaN epitaxial growth, the surface morphology and the influence of polycrystalline particles on selective growth are seldom discussed, however, they play a key role in determining the quality of the devices performance.[20]

In this work, a thick AlGaN capping layer of AlGaN/GaN micro-pyramid is grown by selective MOVPE and the associated polycrystalline particles are formed on a dielectric mask. It is shown that a large amount of surface wrinkling emerges at the bottom of the AlGaN/GaN micro-pyramid, the length of which changes with Al composition. In order to explain the phenomenon of the surface wrinkling, the model of the source supply during SAG is introduced and the effect of the polycrystalline particles on the mask is discussed. The surface diffusion lengths of Ga adatoms along the $\{1\bar{1}01\}$ AlGaN facet are estimated with different Al composition and the nonuniform distribution of Al compositions is characterized by micro-photoluminescence (μ-PL) spectra.

2. Experiment details

The AlGaN/GaN micro-pyramids were grown on a patterned template by using a low pressure MOVPE system according to the following steps. An GaN/AlN film with a thickness of 500 nm/100 nm was grown on the cleaned Si substrate at 1095 °C, which served as a seeding layer for subsequent re-growth. Then, the wafer was taken out from the reactor chamber and a 100-nm-thick SiO_2 was deposited on the seeding layer by plasma-enhanced chemical vapor deposition (PECVD). Afterwards, the SiO_2 mask layer was patterned by conventional photolithography technique and the circle window used as SAG was opened by selective wet etching with diameter and period being 5 μm and 60 μm, respectively. After chemical cleaning, the patterned template was reloaded into the MOVPE chamber for re-growth. The GaN micro-pyramids were first grown on the windows for 30 min at 1020 °C, followed by a 1500-nm-thick AlGaN layer formed on the GaN pyramids at 1080 °C. During the growth, trimethylgallium (TMG), trimethylaluminum (TMA), and NH3 were used as the precursors. The composition content of the $Al_xGa_{1-x}N$ alloy was regulated by changing the flux ratio between TMG and TMA. The surface morphology of the AlGaN/GaN micro-pyramid was characterized by scanning electron microscope (SEM Hitachi S-4800) and atomic force microscope (Veeco Dimension Edge) with an acceleration voltage of 5 kV.

3. Results and discussion

Figure 1 shows the typical GaN and AlGaN/GaN micro-pyramids. The atomic configuration of GaN indicates that the *C* axis and $\langle 1100 \rangle$ axis of the GaN are along the $\langle 111 \rangle$ and $\langle 112 \rangle$ axes of the Si, respectively. The angle between (0001) surface and the sidewalls is 62°, indicating that the sidewalls are all $\{1\bar{1}01\}$ planes. It is shown that the faultless structure with six mirror-like sidewalls is observed when the GaN micro-pyramid is grown, without any polycrystalline particle deposited on the mask. However, after a 1500-nm-thick AlGaN capping layer grown on the GaN pyramids, some surface wrinkling appears at the bottom of the sidewalls but leaving the top part of the pyramid mirror-like. Except for the obvious surface wrinkling, plenty of polycrystalline particles are also observed on the SiO_2 mask.

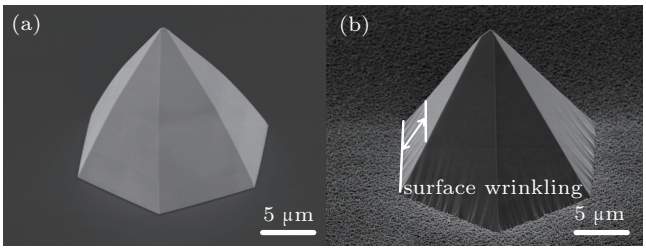


Fig. 1. SEM images of (a) GaN micro-pyramid and (b) AlGaN/GaN micro-pyramid.

In order to reveal the formation mechanism of the surface wrinkling, source diffusion path for selective MOVPE should be illustrated clearly, particularly when the source is transported near the dielectric surface. In selective MOVPE, two main source supply paths are considered.[21] As illustrated in Fig. 2, the first one is the vertical vapor-phase diffusion (VVD) by which the source molecules are directly pushed to the substrate from the ceiling. The second one is the lateral surface migration from the mask region (MMR) by which the source molecules laterally migrate from the dielectric mask region to the growth region. However, large difference in MMR effect exists during the chemical reactions between the GaN and AlGaN compounds on SiO_2. Actually, the material epitaxy was a dynamic equilibrium process of growth and decomposition. In the process of SAG, because of homoepitaxial GaN in the growth region, the growth rate is considerably larger than the decomposition rate and, therefore, GaN pyramids form gradually; whereas, on the SiO_2 surface, the nucleation becomes much harder due to the larger heterogeneous nucleation energy and the decomposition rate is greater than the growth rate. Finally, Ga adatoms could easily migrate to the growth region by VDD and MMR effect, without any polycrystalline particle deposition on the dielectric mask. However, as AlGaN grows, the high bond energy of Al–N prohibits the AlGaN from decomposing under the growth temperature, and the Al adatoms could only migrate freely to the growth region by VDD effect, with some Al adatoms supplied by MMR effect sticking on the SiO_2 surface. Consequently, the GaN micro-pyramids with clean dielectric mask are formed by SAG, and after the AlGaN capping layer is grown on GaN micro-pyramid, the as-

sociated AlGaN polycrystalline particles appear on the surface of the dielectric mask.

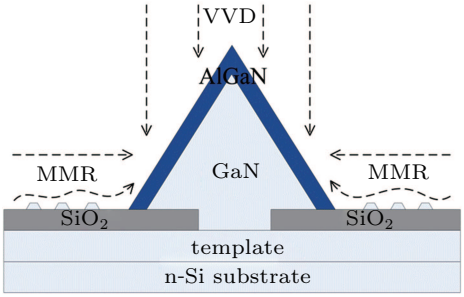


Fig. 2. (color online) Diagram of the source supply paths in selective MOVPE.

It is noted that epitaxy growth is sensitive to the environment of temperature, ambient gas pressure, and flow of source. When polycrystalline particles grow to a considerable scale, the effect related to source supply in selective MOVPE should be considered. Because of the irregular distribution of AlGaN polycrystalline islands on the mask, the source supply from mask regions to growth regions is disturbed and nonuniform. More specifically, a relatively large polycrystalline island on the dielectric mask will slightly block the source from being supplied from the dielectric mask to the growth region, namely the MMR effect near the mask surface, leaving less source supply to the back of the island and more to the side of the island. Therefore, the nonuniform source supply causes the unsymmetrical growth and some surface wrinkling to emerge spontaneously. However, this nonuniform source supply model does not work for the VVD effect, because the VVD effect can directly push the source to the growth region from the ceiling. Furthermore, the MMR effect is the major source supply to the sidewalls of the AlGaN/GaN micro-pyramids but the VVD effect is the major source supply to top regions. As a result, the surface wrinkling shown in Fig. 2, appears at the bottom but leaving the top area symmetrical. Comparatively, GaN micro-pyramids with mirror-like facets, are successfully obtained, because of no polycrystalline islands on the mask.

It is shown that when the AlGaN polycrystalline islands on the dielectric mask are large enough, the nonuniform source supply effect becomes obvious. Therefore the scale of the polycrystalline islands and its influence on the pyramids surface must be discussed. Figure 3 illustrates the high magnification SEM images of AlGaN/GaN micro-pyramids. In this case, the TMA and TMG flow rate are kept at 5×10^{-6} mol/min and 6.5×10^{-5} mol/min, respectively, and the growth time of AlGaN changes from 2 min to 8 min. It is obvious that in the initial growth stage of AlGaN epilayers with a growth time of 2 min, the average size of the polycrystalline particles on the dielectric mask is only about 20 nm characterized by AFM measurements. It is too small to affect the source supply of MMR effect and mirror-like sidewalls appear on AlGaN/GaN micro-pyramids. However, increasing growth time of AlGaN capping layer to 6 min as shown in Fig. 3(c), the polycrystalline particles aggregate into individual islands, with an average size of about 50 nm. Some tiny surface wrinkling is raised at the bottom of the AlGaN/GaN micro-pyramids. As shown in Fig. 3(d), further increasing growth time to 8 min, the surface wrinkling becomes prominent, with larger islands (about 160 nm) appearing on the mask. Our results suggest that the polycrystalline islands play an important role in the migration behaviors of adatoms in selective MOVPE and the effect of polycrystalline islands on source supply should be taken into account when the average scale of the islands on the dielectric mask is larger than 50 nm.

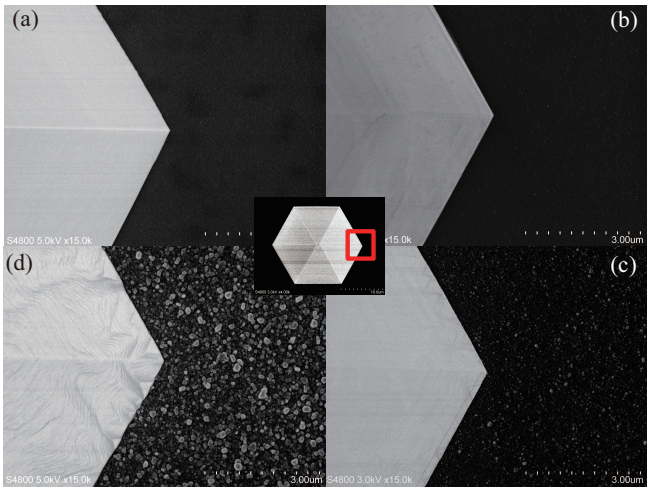


Fig. 3. (color online) SEM images of the AlGaN/GaN micro-paramids with the growth time of GaN for 20 min and AlGaN for (a) 2 min, (b) 4 min, (c) 6 min, (d) 8 min. Insert illustrates the measurement configuration.

The above analysis reveals that the origination of the surface wrinkling arises from the nonuniform migration behaviors of adatoms. Therefore, the scale of the surface wrinkling represents the interaction area where the nonuniform source can reach from the bottom to the top, which is the migration length along the AlGaN $\{1\bar{1}01\}$ facet. Actually, the migration lengths of Al and Ga adatoms show a tremendous difference. The Al adatoms hardly migrate on the semiconductor surface but for the Ga adatoms its migration length is more than several microns[21] and so the length of surface wrinkling apparently indicates the migration length of the Ga adatoms along the AlGaN $\{1\bar{1}01\}$ facet. In order to measure the migration length of Ga adatoms with the change of the composition content of AlGaN, we vary the flow rate of TMA but fix that of TMG. Figure 4 shows the AlGaN/GaN micro-pyramids. The GaN core with six mirror-like sidewalls is performed on the windows for 30 min at 1020 °C. Then the AlGaN capping layer is grown for 30 min at 1080 °C, with the TMA flow

rate changing from 5×10^{-6} mol/min to 4×10^{-5} mol/min and fixing the TMG flow rate at 6.5×10^{-5} mol/min. It is shown that when the TMA flow rate is 4×10^{-5} mol/min, the surface wrinkling is at the bottom of the AlGaN/GaN micro-pyramids, stretching up to $\sim$ 1.5 μm (shown in Fig. 4(b)). Meanwhile, lowering the TMA flow rate, surface wrinkling is stretched up to the top of the pyramid. Particularly, when the TMA flow rate is 5×10^{-6} mol/min, the length of the surface wrinkling increases to $\sim$ 11.8 μm, accounting for three-fourths of the pyramids (shown in Fig. 3(e)). Moreover, the length of the surface wrinkling on GaN $\{1\bar{1}01\}$ facet is also measured. Firstly, the AlGaN/GaN samples with some polycrystalline islands on the mask are obtained. Then the TMG flow rate is settled at 6.5×10^{-5} mol/min and a new GaN capping layer is grown for 5 min on the AlGaN/GaN samples. Figure 4(f) shows the morphologies of the GaN/AlGaN/GaN micro-pyramids. The surface wrinkling covers all the samples, proving that the migration length of Ga adatoms along GaN $\{1\bar{1}01\}$ facet is longer than the length of the sidewalls (16.3 μm).

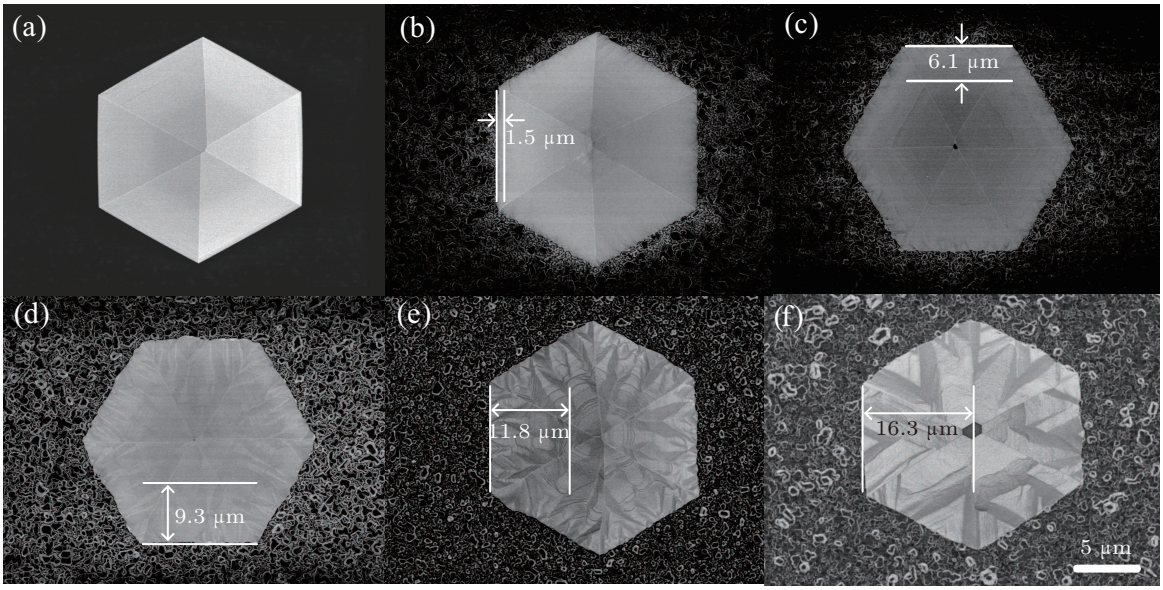


Fig. 4. SEM images of (a) GaN micro-pyramids (b) AlGaN/GaN micro-pyramids with Al flow 4×10^{-5} mol/min, (c) AlGaN/GaN micro-pyramids with Al flow 2×10^{-5} mol/min, (d) AlGaN/GaN micro-pyramids with Al flow 1×10^{-5} mol/min, (e) AlGaN/GaN micro-pyramids with Al flow 5×10^{-6} mol/min, and (f) GaN/AlGaN/GaN micro-pyramids with GaN capping layer grown for 5 min.

The results imply that the migration length of Ga adatoms along the AlGaN $\{1\bar{1}01\}$ facet is estimated to be in a range from 1.5 μm to larger than 16 μm in our experimental condition and changes inversely proportional to the TMA flow rate. Although the migration ability of Al atom is much lower than that of Ga adatoms, the interactions combine two adatoms into an integrated cluster. The increasing of Al composition content strengthens bound energy of AlGaN and makes the decomposition harder, which enlarges the bound ability of adatoms, leading to less migration length of Ga species on the AlGaN $\{1\bar{1}01\}$ facet. Those results are in agreement with the conclusion previously reported by other groups.[18] This surface wrinkling on GaN/AlGaN/GaN micro-pyramids further confirms the initial conclusion that the irregular distribution of AlGaN islands on the mask disturbs the migration of source material, leading to the irregular material growth.

For investigating the compositional uniformity of the AlGaN capping layer, the optical characteristics of the AlGaN/GaN micro-pyramids are obtained by room temperature micro-photoluminescence (μ-PL) measurement. The AlGaN capping layer is grown for 30 min at 1080 °C by supplying TMG $= 6.5\times10^{-5}$ mol/min, TMA $= 1\times10^{-5}$ mol/min, of which the μ-PL spectra are shown in Fig. 5. The measurements are performed from the apex to the dielectric mask with a laser spot of 5 μm in diameter in four steps. The μ-PL spectra show three emission peaks, which are at 369 nm, 353 nm, and 338 nm, corresponding to GaN band-edge emission and $Al_xGa_{1-x}N$ emission for $x = 6\%$ and 13.8%, respectively. When the laser spot is focused on the apex, PL spectrum with a dominant GaN-emission peak and a weaker 355 peak is observed. As the laser spot is moved to the middle part of a side facet, three peaks are observed in the spectrum. Further shifting the laser spot to the bottom of the micro-pyramids, only one main peak at 338 is observed, which is consistent with the emission of the polycrystalline islands on the dielectric mask. The variations of PL spectrum with excitation position of laser spot moving indicates that the Al composition content in the bottom of the AlGaN capping layer is larger than that in the top part. Actually, the Al composition content of the polycrystalline islands on the dielectric mask and the bottom of the pyramids, consists with that in the vapor phase. However, as the species migrate from the bottom to the top part by

MMR effect, more Ga adatoms will migrate to the top of the AlGaN capping layer than Al adatoms because the atomic migration ability of Ga is larger than that of Al adatoms during the selective area growth. Moreover, also due to the different migration ability, additional Ga source supplied from a larger space span contributes to the growth region, thereby leading to the lower Al composition content on the top of the AlGaN capping layer.

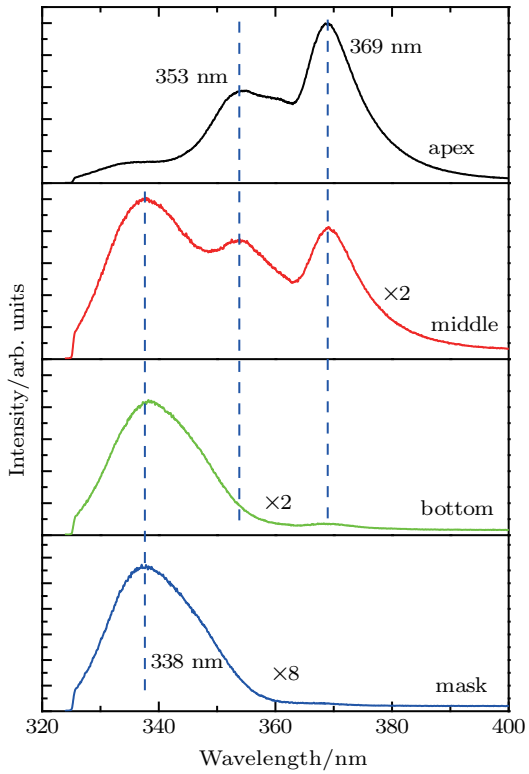


Fig. 5. (color online) Room temperature μ-PL spectra of AlGaN/GaN micro-pyramid performed on different places.

4. Conclusions

In this work, AlGaN/GaN micro-pyramids grown by selective MOVPE are studied. It is shown that a large amount of surface wrinkling emerges at the bottom of the AlGaN/GaN micro-pyramid, which is caused by the nonuniform source supply from the dielectric mask region to the growth region when the scale of the polycrystalline particles on the mask is larger than 50 nm. Analysis clarifies that the size of surface wrinkling is related to the migration length of Ga adatoms along the AlGaN $\{1\bar{1}01\}$ facet, and is enhanced by reducing the TMA flow rate. Multi-color emission from the AlGaN/GaN micro-pyramid is observed by μ-PL, and the compositional variation of Al originates from the additional Ga source supply due to its larger atomic migration length. Therefore, it may be possible to fabricate compositional uniformity of the AlGaN layer by eliminating the difference in atomic migration length between Ga and Al.

References

[1] Xie J, Mita S, Bryan Z, Guo W, Hussey L, Moody B, Schlesser R, Kirste R, Gerhold M and Collazo R 2013 *Appl. Phys. Lett.* **102** 171102
[2] Grandusky J R, Gibb S R, Mendrick M C, Moe C, Wraback M and Schowalter L J 2011 *Appl. Phys. Express* **4** 082101
[3] Taniyasu Y, Kasu M and Makimoto T 2006 *Nature* **441** 325
[4] Zhang C, Sun H Q, Li X N, Sun H, Fan X C, Zhang Z D and Guo Z Y 2016 *Chin. Phys. B* **25** 028501
[5] Khan M A, Shatalov M, Maruska H P, Wang H M and Kuokstis E 2005 *Jpn. J. Appl. Phys.* **44** 7191
[6] Hirayama H 2005 *J. Appl. Phys.* **97** 091101
[7] Floro J A, Follstaedt D M, Provencio P, Hearne S J and Lee S R 2004 *J. Appl. Phys.* **96** 7087
[8] Lee S R, Koleske D D, Cross K C, Floro J A, Waldrip K E, Wise A T and Mahajan S 2004 *Appl. Phys. Lett.* **85** 6164
[9] Shatalov M, Sun W, Lunev A, Hu X, Dobrinsky A, Bilenko Y, Yang J, Shur M, Gaska R, Moe C, Garrett G and Wraback M 2012 *Appl. Phys. Express* **5** 082101
[10] Yang W, McPherson S A, Mao Z, McKernan S and Carter C B 1999 *J. Cryst. Growth* **204** 270
[11] Kawaguchi Y, Honda Y, Matsushima H, Yamaguchi M, Hiramasu K and Sawaki N 1998 *Jpn. J. Appl. Phys.* **37** L966
[12] Xiao H P, Chen Y P, Yang K K, Wei X L, Sun L Z and Zhong J X 2012 *Acta Phys. Sin.* **61** 178101 (in Chinese)
[13] Ren P, Han G, Fu B L, Xue B, Zhang N, Liu J, Zhao L X, Wang J X and Li J M 2016 *Chin. Phys. Lett* **33** 068101
[14] Srinivasan S, Stevens M, Ponce F A and Mukai T 2005 *Appl. Phys. Lett.* **87** 131911
[15] Chen W J, Han X B, Lin J L, Hu G H, Liu M G, Yang Y B, Chen J, Wu Z S, Liu Y and Zhang B J 2015 *Chin. Phys. B* **24** 118101
[16] Hiruma K, Haga T and Miyazaki M 1990 *J. Cryst. Growth* **102** 717
[17] Kozawa T, Ohwaki T and Taga Y 1999 *Appl. Phys. Lett.* **75** 3330
[18] Narita T, Honda Y, Yamaguchi M and Sawaki N 2006 *Phys. Stat. Sol. (b)* **243** 1665
[19] Honda Y, Torikai M, Nakamura T Y. Kuroiwa, M. Yamaguchi and N. Sawaki 2003 *Phy. Stat. Sol. (c)* **70** 2043
[20] Arjunan A C, Singh D, Wang H T, Ren F, Kumar P, Singh R K and Pearton S J 2008 *Appl. Surf. Sci.* **255** 3085
[21] Sakata Y, Inomoto Y and Komatsu K 2000 *J. Cryst. Growth* **208** 130